Numerical Simulation of the Toner Melting Behavior in Fuser Nip Considering Toner Rheology

Satoshi Hasebe; Key Technology Lab, Fuji Xerox Co., Ltd.; Nakai, Kanagawa, Japan

Abstract

New numerical method to compute toner melting behavior in the fuser nip was developed by combining the recently proposed CCUP method known as a general solver for gas, liquid and solid and the Leonov model as a rheological model. In present method, deformation of the piled up powder toners by heat and load were computed using the fitted dynamic property of the viscoelastic parameters: G', G" and the WLF equation. In this study, effects of the fusing temperature, the nip load and the process speed on melting behavior were investigated. Consequently, the computed toner pile height and the surface roughness show good correspondence with experimental ones, and the validity of the present method was demonstrated.

Introduction

Fusing process consumes about 70% of the total machine power. Therefore new fuser system with low power and high productivity is required to meet severe environmental standard. Fusing performances such as bond strength and gloss are controlled by the fusing temperature, the nip pressure profile and the process speed, each affects on toner melting behavior. Therefore, it is important to clarify effects of these fusing parameters on the fusing performance.

Toner melting process in the fuser nip is governed by multi-physics problem with reciprocal interaction; dynamics of the rigid and the elastic material, toner rheology with phase change, air flow among toner particles and heat conduction. And it has also free surface problem; the surface and inner shapes of the toner change with merge and stretch by melt. For these difficulties, there have been few studies treating the toner melting process in fuser nip directly by the numerical approach. In present study, to overcome these problems, CCUP(CIP-Combined and Unified Procedure) method [1] is selected because this method is able to treat solid, liquid and gas simultaneously and also track deforming interface with high accuracy in Eulerian grid without numerical diffusion and mesh crash. As for toner rheology, the Leonov model considering dynamic viscoelastic properties of the toner is employed [2] and coupled with CCUP method to compute interactions simultaneously. As the temperature model for viscoelastic properties, WLF (Williams-Landel-Ferry) equation is used.

In present report, the outline of the present method is explained and its validity is demonstrated for various fusing condition (temperature, nip load and process speed) .

Target Fuser System

The target fuser for toner melt simulation is the roller-belt type fuser (Free Belt Nip Fuser)[3], which can create wide nip width, illustrated in Fig.1. The soft pressure pad plays a role of melting toner with low pressure, and the hard pad realizes a high peeling performance. The pressure profile in the process direction is also depicted in Fig.1.

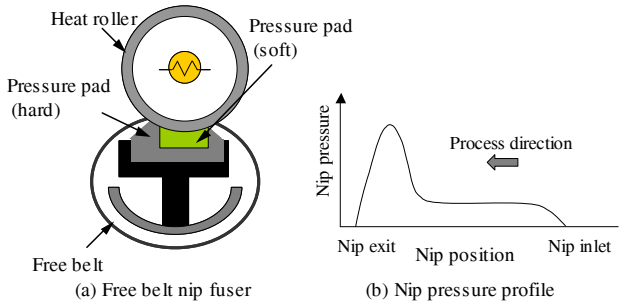

Figure 1. *Sketch of Free belt nip fuser and pressure profile across the nip width*

Numerical Method

CCUP Method

Set of the hydrodynamic equation is described in Eq.1. The components are continuity equation of mass, equation of motion, equation of pressure and energy balance equation:

$$\frac{\partial \mathbf{f}}{\partial t} + (\mathbf{u}\cdot\nabla)\mathbf{f} = \mathbf{g}\,, \tag{1}$$

where, $\mathbf{f} = \begin{bmatrix} \rho \\ \mathbf{u} \\ p \\ T \end{bmatrix}$, $\mathbf{g} = \begin{bmatrix} -\rho\nabla\cdot\mathbf{u} \\ (-\nabla p + \nabla\sigma)/\rho + \mathbf{F} \\ -\rho C_s{}^2 \nabla\cdot\mathbf{u} \\ \nabla\cdot(\lambda\nabla T)/\rho C_p \end{bmatrix}$,

ρ :density, $\mathbf{u}$:velocity vector, p :pressure, T :temperature, σ :stress tensor of the viscosity, elasticity and viscoelasticity, etc., $\mathbf{F}$:body force, C_s :acoustic speed, λ :heat conductivity, C_p :specific heat at constant volume.

The CCUP method employs time splitting method; Eq.1 is split into advection phase on the left and non-advection phase on the right in Eq.2:

$$\frac{\partial f^*}{\partial t} + (\mathbf{u}\cdot\nabla)\mathbf{f} = 0\,,\quad \frac{\partial f^{**}}{\partial t} = \mathbf{g} \tag{2}$$

In non-advection phase, Poisson's equation of the pressure given by Eq.3 without stress term is solved by finite difference method.

$$\nabla\left(\frac{\nabla p^*}{\rho^n}\right) = \frac{p^* - p^n}{\rho C_s{}^2 \Delta t^2} + \frac{\nabla\cdot\mathbf{u}^n}{\Delta t} \tag{3}$$

The equation of motion is solved following the time splitting procedure using the intermediary value of the velocity. After calculating the non-advection phase, advection equation in Eq.2 is

solved to get the values of the next time step as the final procedure. The interface of different materials is automatically identified by introducing color function by each material whose value has 1 in the occupied area and 0 otherwise. The time evolution of the interfaces is tracked by solving the advection equation of the color functions: ϕ_m using the digitizer (tangent transformation) that restrains interface diffusion:

$$\frac{\partial F(\phi_m)}{\partial t} + \mathbf{u} \cdot \nabla F(\phi_m) = 0, \quad m = 1,2,...,M \tag{4}$$

Adevection equations in Eq.2 and Eq.4 are solved using the CIP method[1]. The CIP method has performance of third order accuracy with both time and space. The feature is that advection equation of the gradient of the physical value is also solved to keep its spatial profile from numerical diffusion. The profile between two grid points is interpolated by cubic function. Figure 2 demonstrates the performance of the CIP method. Suppose the rectangle profile of concentration $(10 \le x \le 20)$ propagates downward with constant velocity: $u = 0.5$. Here grid space: $\Delta x = 1$, time step: $\Delta t = 0.02$. CIP method maintains the initial profile after 800 iterations, while conventional first order up-wind scheme dissipates its initial profile by the numerical diffusion.

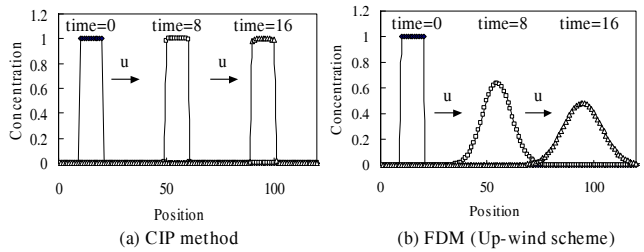

***Figure 2**. Simulation result of the CIP method and the conventional finite difference method (up-wind scheme) for the advection equation*

Rheological Model

The Leonov model[2] is described by the parallel connections of the Maxwell element, the spring and the dashpot in series, and a dashpot as illustrated in Fig.3. The constitutive equation is given by Eq.5:

$$\sigma = 2\sum_{k=1}^{m} \frac{\partial W_k}{\partial \mathbf{I}_{k,1}} \mathbf{c}_k + 2\sum_{k=1}^{m} \frac{\partial W_k}{\partial \mathbf{I}_{k,2}} \mathbf{c}_k^{-1} + 2\eta_0 s\dot{\gamma}\mathbf{e} \tag{5}$$

where σ :stress tensor, subscript k :relaxation mode, W :elastic potential, $\mathbf{c}$:reversible Finger's elastic strain tensor, I_1, I_2 :first and second invariants of $\mathbf{c}$, $\dot{\gamma}$:rate of strain, $\mathbf{e}$:rate of strain tensor, s :dimensionless rheological parameter, η_0 :zero shear viscosity, ω :vorticity tensor, $\mathbf{e}_p$:irreversible rate of strain tensor, W :elastic potential in Neo Hookean assumption, G :Hookean modulus, η :Newtonian viscosity, τ :relaxation time.

The form of the elastic potential is given by:

$$W_k = \frac{G_k}{2}(I_{k,1} - 3), \quad G_k = \eta_k / \tau_k \tag{6}$$

Simultaneous equations of each component of $\mathbf{c}$ given by Eq.7 to Eq.9 are implicitly solved for each relaxation mode:

$$2\tau_k \frac{dc_{11,k}}{dt} + c_{11,k}^2 - 1 + c_{12,k}^2 = 4\tau_k \dot{\gamma} c_{12,k} \tag{7}$$

$$2\tau_k \frac{dc_{12,k}}{dt} = 2\tau_k \dot{\gamma} c_{22,k} - c_{11,k} c_{12,k} - c_{12,k} c_{22,k} \tag{8}$$

$$c_{11,k} c_{22,k} = 1 + c_{12,k}^2 \tag{9}$$

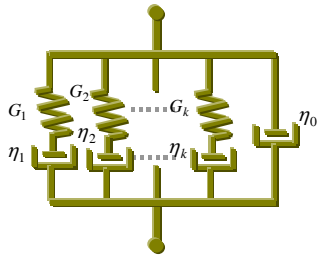

***Figure 3**. Schematic diagram of the Leonov model*

Reproduction of Viscoelastic Properties

The storage modulus: G' and the loss modulus: G'' for frequency sweep are fitted by optimizing the viscosity and the relaxation time using the theoretical formulae of the generalized Leonov model:

$$G'(\omega) = \sum_{k=1}^{N} \frac{\eta_k \tau_k \omega_k^2}{1 + \tau_k^2 \omega_k^2}, \quad G''(\omega) = \sum_{k=1}^{N} \frac{\eta_k \omega_k}{1 + \tau_k^2 \omega_k^2} + s\eta_0 \omega \tag{10}$$

As for the temperature sweep, the WLF equation given by Eq.11 is used at arbitrary temperature applying the relations described in Eq. 12.

$$\log(a_T) = -\frac{C_1 (T - T_{ref})}{C_2 + T - T_{ref}} \tag{11}$$

$$\tau_k(T) = \tau(T_{ref}) a_T, \quad \eta_k(T) = \eta(T_{ref}) a_T \tag{12}$$

where a_T :shift factor, T_{ref} :reference temperature, C_1, C_2 : constants.

Toner Melt Simulation

Simulation model

Two-dimensional section of the fuser nip across the axis is considered including six materials: Aluminum core shaft, elastic layer (Si-rubber), surface layer (PFA), toner, ambient air and paper as shown in Fig.5. The time evolution across the process direction is computed with nip load. Suppose that heat roller and paper are rigid body and have flat surface, and toner is chemical toner on market whose particle has round shape with diameter of $6\,\mu m$. The temperature of toner, air and paper is set at $30\,^{\circ}C$ and that of heat roller is set at fusing temperature as an initial condition. Top boundary is maintained at a fusing temperature, the bottom, left and right side are in adiabatic condition respectively. The number of the relaxation mode for the viscoelastic calculation is four and rheological parameter in Leonov model: $s = 0$. Any adhesive force is not considered. The computational mesh is non-uniform structured grid. The toner particle is partitioned by 12×12 meshes.

Flow of the calculation is as follows; 1)calculate the 1st fractional step of non-advection phase in CCUP procedure without stress term, 2)calculate the temperature, 3)calculate the shift factor by the WLF equation, 4)calculate the Finger's strain tensor for each relaxation mode and viscoelastic stress in the Leonov model, 5)calculate the 2nd fractional step of non-advection phase by

explicitly coupling the viscoelastic force with CCUP procedure, 7) calculate the advection phase by the CIP method and update physical values, 8)go to the next time step

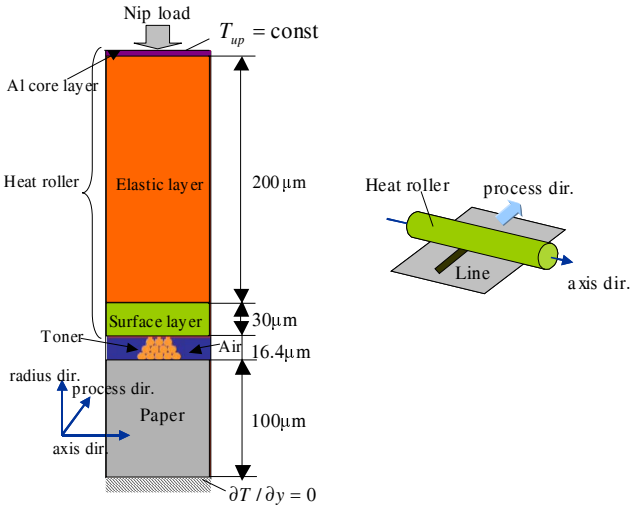

Figure 5. *Simulation model of the fuser nip*

Toner Melting Process

Figure 6 shows the snapshots of the toner melting process in different fusing temperature. In Fig.6, only the upper toner particles contacting with the heat roller soften to deform by compression, and then the surface toners stretches outward as the elasticity decreasing. In contrast, the toner near the paper interface keeps granulation because of the temperature gap. As the heat conducts to the bottom, enhancement of stretching and merging of toners occurs by the nip load.

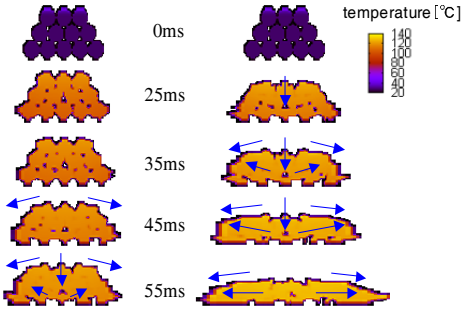

(a) Low fusing temperature (b) High fusing temperature

Figure 6. *Comparison of the toner melting process for different fusing temperature*

Figure 7 demonstrates the TEM image of the fused toner section for reference. A and B in Fig.7 indicates low and high temperature case, respectively. Although the fusing condition is different from the computation, the computed surface shapes at 55ms in Fig.6 and the observed ones shows good correspondence for the different temperature case.

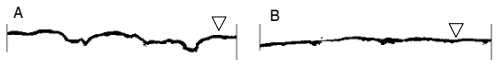

(a) Low fusing temperature (b) High fusing temperature

Figure 7. *Observation of the fused toner surface shapes for different fusing temperature*

Accuracy Verification for Fusing Parameters

Demonstrating the performance of the present method, simulated toner pile height at the exit of the nip is compared with the experimental ones for various fusing parameters: Fusing temperature(150,170,190 ℃), process speed(104,165,208mm/s), amount of toner(two and three layer). The target fuser type is the Free Belt Nip Fuser. In this simulation, composition of toner is different from prior case. Figure 8 shows the final shapes of the fused toner computed.

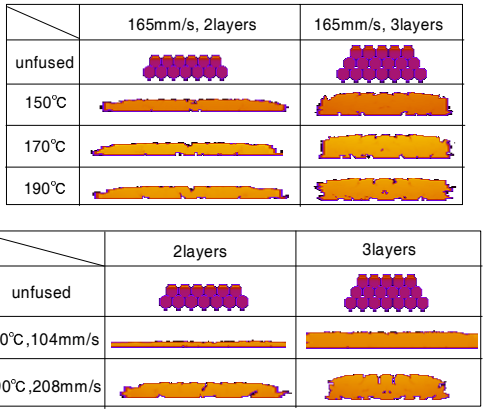

Figure 8. *Simulated fused toner shape for various fusing parameters*

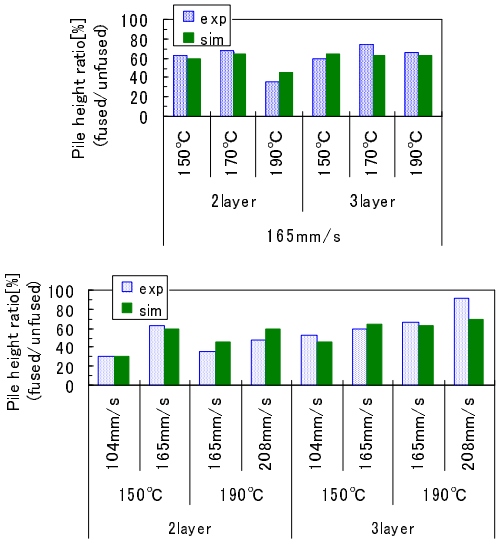

Figure 9. *Comparison of the fused toner pile height ratio between experiment and simulation for various fusing parameters*

Figure 9 indicates the comparison of the pile height ratio(fused/unfused) between experiment and simulation results. The averaged pile height over the length of 100 to 150 μm measured by the laser microscope is used. Simulated pile height shows qualitative correspondence to the experimental ones with high correlation over $r = 0.9$ concerning the fusing temperature and the process speed.

Effect of the Fusing Parameters

From the results in cases of the same process speed (165mm/s), almost all pile height ratios are same despite the different fusing temperatures. As for the effect of the process speed, there is a positive correlation between the pile height and the process speed in all cases for each fusing temperature in Fig.9. Low process speed shifts pile height to lower. Figure 10 and 11 plot the history of the pile height and the toner temperature of both the paper and the heat roller interfaces. Figure 10 shows the effect of the fusing temperature(150 and 190 °C) at the constant process speed in three layers of toner. This result suggests that the compression process is almost the same even though the toner temperatures at the interfaces have difference about 20 °C . However surface shape and inner structure of fused toner depend on the fusing temperature as shown in Fig.8.

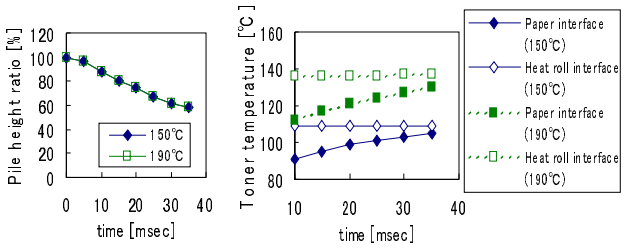

Figure 10. *Change of the toner pile height and toner interface temperature (fusing temperature:150 and 190 °C constant process speed, three layers)*

Figure 11 indicates the case of the process speed 104mm/s at the fusing temperature 150 °C and that of 208mm/s at 190 °C . In this case, the nip load profile across the nip width is same, but the time history of that is different according to the process speed. In Fig.11, the pile height in the case of 104mm/s at 150 °C is about two times lower than that of 208mm/s at 190 °C although the toner temperature is lower more than 20 °C . This result shows that the toner melt does not depend only on temperature and implies the importance of the loading time and the dynamic property of the nip load for toner melt from the viewpoint of the toner rheology.

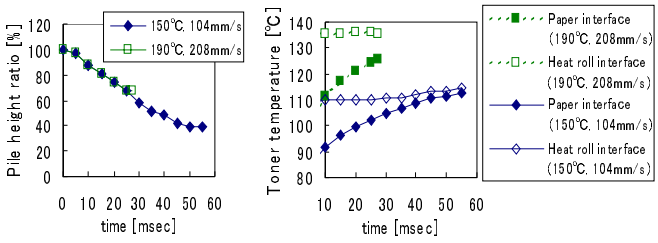

Figure 11. *Change of the toner pile height and toner interface temperature (104mm/s at 150 °C case and 208mm/s at 190 °C case, three layers)*

Effect of the Nip Load

Figure 12 plots the time history of the pile height ratio(fused /unfused) and the temperature difference between top and bottom interface of the toner with/without constant nip load of 0.15MPa, at the fusing temperature of 170 °C . This result shows that the nip load promotes toner melt and decreases the temperature gap by the compression of the toner layer.

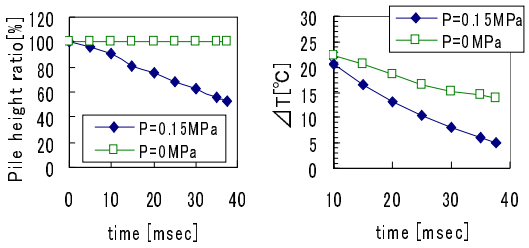

Figure 12. *Time history of the toner pile height ratio and temperature difference between top and bottom surface of the toner*

Conclusion

New technique for direct computation of the toner melting process in the fuser nip has been developed. This technique enabled to compute the effect of the nip load on toner melt and the dynamics of air among toner particles. The features of the present method were as follows; 1)Consider toner rheology by employing the four mode Leonov model considering viscoelastic properties for temperature by the WLF equation, 2) Employ the CCUP method for computing the multi-physics and free surface problem.

Validity of the present method was demonstrated for various fusing parameters. The high positive correlation over $r = 0.9$ was observed with the experimental results as to the toner pile height.

And interesting results were obtained that the time histories of the toner pile height were almost the same for different fusing temperature. This result implies the importance of the loading condition for the toner melting process.

In the future study, we will clarify the fusing mechanism and stripping behavior from the viewpoint of the toner rheology.

Acknowledgements

The author is grateful to Y.Naito, M.Baba and A.Kakishima for their cooperation in the experiment.

References

[1] T.Yabe, F.Xiao and T.Utsumi, “The Constrained Interpolation Profile Method for Multiphase Analysis”, Int. J. Compu. Phys., 169, 556, (2001).

[2] A. I. Leonov, E. H. Lipkina, E. D. Paskhin and A. N. Prokunin, “Theoretical and experimental investigation of shearing in elastic polymer liquids”, Rheologica Acta, 15, 411-426, (1976).

[3] http://www.fujixerox.co.jp/company/technical/fbnf/index.html

Author Biography

Satoshi Hasebe received his BS(1991), MS(1993) and Dr. degree (1997) in mechanical engineering from Hokkaido University (Japan). Since then he has worked in the Key Technology Laboratory at Fuji Xerox. His work has focused on the development of the simulation techniques for electrophotography. He is a member of Imaging Science of Japan and Japan Society of Mechanical Engineering